Aquacultural Engineering 42 (2010) 103–111

Contents lists available at ScienceDirect

Aquacultural Engineering

journal homepage: www.elsevier.com/locate/aqua-online

The use of an open channel, low pressure UV reactor for water treatment in low head recirculating aquaculture systems (LH-RAS)

Hadas Mamane [a,b,*], Angelo Colorni [a,b], Ido Bar [a,b], Ido Ori [a,b], Noam Mozes [a,b]

[a] School of Mechanical Engineering, Tel-Aviv University, Tel Aviv 69978, Israel
[b] Israel Oceanographic & Limnological Research Ltd., National Center for Mariculture, P.O. Box 1212, Eilat 88112, Israel

ARTICLE INFO

Article history:
Received 9 July 2009
Accepted 24 December 2009

Keywords:
Ultraviolet
Recirculation
Aquaculture
Disinfection
Actinometry
Open channel
Water treatment

ABSTRACT

This study examined the effectiveness of an open channel, low pressure (LP), ultraviolet (UV) reactor for water treatment in a low head (LH) recirculating aquaculture system (RAS). Currently available UV reactors use high pressure pumps and submerged bulbs. The reactor in this study makes use of the head gained by the water recirculation of the LH-RAS without the need for additional pumps, while the bulbs are located above water surface to ease maintenance and lower costs. The UV reactor's output was characterized and evaluated by measuring the fluence rate distribution at various *X*, *Y* locations and average UV fluence rate delivered to the water surface using spherical chemical actinometry. The average UV fluence rate measured in dry conditions at the surface of the test water was 2.3 mW cm^{-2}. Measurements of the exponential decay of irradiance in the water with the increase in water depth corresponded well with transmittance results, and were used to estimate the reactor's UV dose at different water flow rates. Using collimated beam apparatus (CBA), the inactivation of heterotrophic microorganisms in the RAS as a function of UV fluence showed that survival of bacteria dropped significantly as the UV dose increased and then stabilized at higher UV doses. Log survival at the UV reactor installed in the RAS was used to back calculate the average UV dose, which resulted to be of ~2 mJ cm^{-2} based of the CBA data, and ~4 mJ cm^{-2} based on dose equations at water flow rates of 100 m^3 h^{-1}. Only a certain amount of sensitive bacteria can be inactivated by fluence rates delivered at UV doses of 2–4 mJ cm^{-2}, thus to increase the delivered UV dose, it is suggested to increase the power of the UV bulbs, and to use this system in water with low transmittance and gravitational flow as in LH-RAS, for the benefit of controlling pathogenic bacteria proliferation.

1. Introduction

The Israeli government's decision to remove two major commercial cage fish farms from the Gulf of Eilat (Red Sea) by June 2008 was followed by a pressing urge to develop an adequate technology for a more environment-friendly, land-based mariculture. The National Center for Mariculture (NCM) in Eilat and Kora Ltd. have been developing and evaluating a low head (LH) marine recirculating aquaculture system (RAS) as a sustainable land-based alternative to cage farming in the sea. In such systems, fish are reared at high densities using a limited inflow of make-up seawater, where the daily effluent discharge is typically 5–50% of the system volume. The overall purpose of the RAS is to minimize consumption of make-up seawater. However, the limited make-up water flow results in accumulation of organic matter, especially particulate, and nitrate (Klas et al., 2006). Thus, all recirculating production systems remove waste solids, oxidize ammonia and nitrite-nitrogen, remove carbon dioxide, and aerate or oxygenate the water before returning it to the fish tank (Losordo et al., 1998). At the NCM, water is treated by recirculating water through a solid filter and biofilters using a low head flow driven by air-lifts (Mozes et al., 2003).

In recirculating systems, various pathogens may develop and threaten the entire culture. Infectious diseases are a major hazard to RAS operations because in such intensive systems they can spread rapidly. Thus, some systems may require also some form of disinfection (Losordo et al., 1998). A possible solution to the microbiological problem lies in devising an efficient, inexpensive disinfection treatment for controlling proliferation of waterborne pathogens circulating in the RAS.

Common treatments widely used for disinfecting water in aquaculture applications are ozone and UV (Summerfelt, 2003). Each system has specific advantages and disadvantages. For example, besides inactivating fish pathogens, ozone can be used to oxidize organic molecules and nitrite, and thus improve water

* Corresponding author at: School of Mechanical Engineering, Faculty of Engineering, Tel-Aviv University, Tel Aviv 69978, Israel.
E-mail address: hadasmg@post.tau.ac.il (H. Mamane).

0144-8609/$ – see front matter © Elsevier B.V. All rights reserved.
doi:10.1016/j.aquaeng.2009.12.005

quality; while oxygenating the water, however, it may leave toxic residues that must be removed before reaching aquatic organisms, and may produce noxious disinfection byproducts such as brominated organics and inorganics and trihalomethanes (THMs). Finally, ozone production is expensive (Summerfelt, 2003). Another way of controlling pathogens is using UV radiation to disinfect water within the system. UV disinfection has gained growing acceptance as a primary disinfection process for water since it was found to be very effective for inactivating *Cryptosporidium* (Clancy et al., 2000; Craik et al., 2001; Shin et al., 2001) and *Giardia lamblia* (Linden et al., 2002), two protistan pathogens, without forming residual disinfection byproducts produced with oxidative disinfectants. A drawback relates to water quality, as in the RAS water is rich in particulate matter and this results in decreased UV penetration and treatment effectiveness (Mamane, 2008).

Kornmueller (2007), however, stated that due to the wide diversity of marine microorganisms (viruses, bacteria and algae) no single disinfectant is actually capable of neutralizing all of them at once, and presented the advantages of using advanced oxidation processes (AOPs). AOPs are processes involving the accelerated production of hydroxyl radicals (Singer and Reckhow, 1999). Combining ozone and UV irradiation, as an AOP process, could be used to disinfect an entire recirculating flow before it returns to the fish tank (Sharrer and Summerfelt, 2007).

Current technology for water disinfection by UV includes two basic types of mercury lamps: low pressure (LP) UV mercury vapor lamps that emit single monochromatic wavelength that peaks at 253.7 nm, and medium pressure (MP) UV mercury lamps with a broad polychromatic spectrum with output at multiple wavelengths throughout the 220–300 nm germicidal UV range and beyond. Full-scale drinking water applications generally use LP, low-pressure high output (LPHO), or MP mercury vapor lamps (USEPA, 2006). LP lamps are used in water treatment plants due to the high efficiency at the microbicidal wavelength without producing unwanted photochemical changes in other water constituents (Chiu et al., 1999; Haider et al., 2002).

Radiometry, a common method of irradiance measurement, is not suitable for measuring the irradiation in a UV reactor, from an array of UV sources, nor with scattering suspensions, because the radiometer measures irradiation normal to the planar surface of the detector (Rahn et al., 1999). Proper fluence rate measurement – the total radiant power from all directions onto an infinitesimally small sphere – can be approximated using an experimental tool that receives UV photons from different directions (Rahn et al., 1999; Bolton, 2001). One extensively used alternative to traditional radiometry is chemical actinometry, which is a chemical method that measures a chemical change produced by radiation. The decrease in concentration of actinometer upon exposure to either monochromatic or polychromatic UV sources is utilized to directly calculate the UV fluence. Examples for actinometers are the iodide/iodate process based on a photochemical reaction sensitive to 254 nm (Jortner et al., 1961; Rahn, 1997) and the potassium ferrioxalate actinometer sensitive to variable wavelengths between 200 and 300 nm (Hatchard and Parker, 1956). In general, any defined photochemical reaction can be used as a chemical actinometer provided that the formation of the photoproduct is straightforward with the number of absorbed photons, and the quantum yields (QY) are accurately known for a large number of wavelengths (Kuhn et al., 1989).

UV disinfection systems consist of UV lamps, quartz sleeves, a structure that supports the lamps and in many cases a cleaning system to maintain transparency of the quartz sleeve. Disinfection systems are classified as either open channel gravity flow systems or closed vessels pressurized systems. With open channel systems, typical for LP lamps, the lamps are placed in modules or racks that are submerged in the flow. Closed vessel systems, typical for most LP, LPHO and MP lamps, operate under pressure, thus they are particularly attractive in upgrades and plant retrofit (Crittenden et al., 2005). Leonard et al. (2000) conducted a study on a RAS system with a UV disinfection unit operating under pressure. Components in a RAS system included an oxygenated fish tank, a particle separator, a 60 μm mechanical filter, a pumping tank, a pump, and the UV disinfection unit that was followed by a biological filter. Leonard et al. (2000) concluded that although fixed biofilms (formed on the biological filter) when released were a main source of free bacteria within the RAS water, the UV disinfection unit was able to keep a stable concentration of free bacteria in the system. Thus UV may be a viable solution to control such free bacterial concentration in the RAS.

Aiming at reducing operational costs, the effectiveness of a different type of UV reactor for water treatment was considered as means for controlling pathogens proliferation. The reactor used in this study was a non-submerged open channel, LP UV reactor that utilizes the low-head gravitational flow pattern of water recirculation of the LH-RAS. This configuration was designed so as to eliminate the need for additional pumps, pressurized pipes, sealing, while placing the lamps above water surface aimed at reducing fouling, easing maintenance and thus lowering costs.

The specific objectives of this study were to (a) characterize the UV reactor's output by measuring the UV fluence rate delivered to the water surface by actinometry, (b) determine the UV fluence rates transmitted through the water under different water depths, (c) perform dose–response curves using a LP UV collimated beam apparatus with bacterial population in the RAS, (d) determine the relationship between circulating water flow rates in the RAS and UV doses to achieve the required dose, and (e) test the impact of the non-submerged LP UV reactor on inactivation of microorganism population in an operating LH-RAS.

2. Methods and materials

2.1. Description of the experimental LH-RAS system

The LH-RAS parameters in which the experimental UV reactor was tested were as follows: RAS tank volume was 100 m^3 covered with green PVC sheets, fish biomass was 3–4 ton (sea-bream, *Sparus aurata*), resulting in rearing density of 30–40 kg m^{-3}, feed intake was 20–40 kg day^{-1}, recirculation flow rate was typically 100 m^3 h^{-1} and make up flow rate was 40–50 m^3 day^{-1} (Mozes et al., 2003). Seawater was pumped from the Red Sea, having a salinity of 40 ppt. Water treatment included the following: a solid filter (static layer with plastic beads), a moving bed biofilter used for nitrification, air lift pump, LP UV disinfection unit that was followed by an oxygenated fish tank. Seawater was continuously fed to the system. A schematic illustration of the RAS is presented below (Fig. 1).

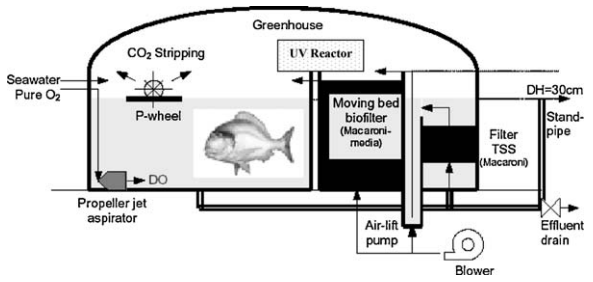

Fig. 1. Schematic configuration of the LH-RAS with the addition of the low pressure ultraviolet (LP-UV) reactor (adapted from Mozes et al., 2003).

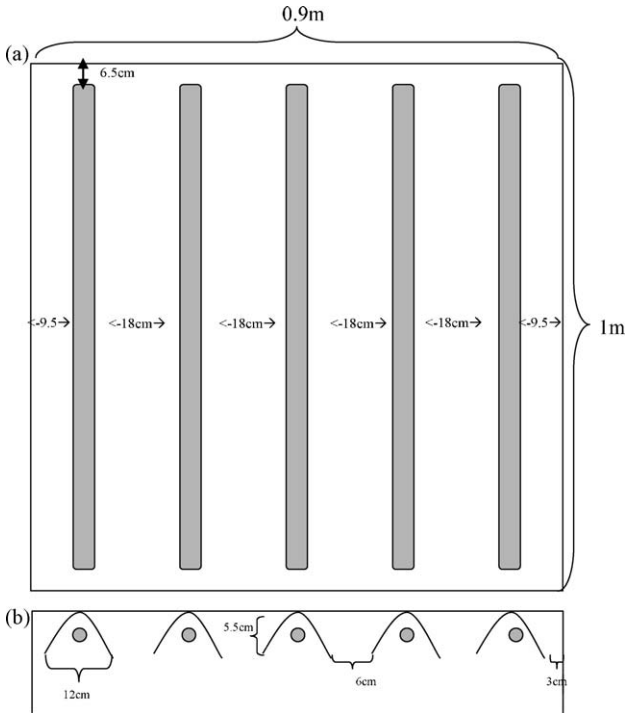

Fig. 2. (a) Top view of the reactor ceiling 1 m wide and 0.9 m long; (b) side view of reflector configuration or the five lamps.

2.2. UV reactor configuration

The UV reactor was designed by Kora Ltd. (Israel). The UV reactor comprised two parts, (a) the rectangular base which included a tray 1 m wide and 0.9 m long, with an opening that allowed water to enter and exit the reactor at a water depth of 10–15 cm, and the tray, corrugated to enhance water mixing, and (b) the reactor ceiling that supported five low pressure (LP) UV lamps emitting monochromatic radiation at 253.7 nm oriented normal to the surface of the test water and situated at equal distances along the reactor, with five reflectors made of polished aluminum that directed the lamp output towards the tray (Fig. 2). The lamps were 30 W each, with 30–40% lamp efficiency and dimensions of 90 cm length, 26 mm diameter and 82 cm arc length (model TUV 30 W T8, Philips). Irradiation zone covered approximately the entire 9000 cm^2 system dimension. Fig. 3 shows a photograph of the UV reactor.

2.3. Methods for actinometry preparation

The iodide/iodate actinometer is based on the following photochemical reaction (Rahn, 1997):

$$8I^- + IO_3^- + 3H_2O + h\nu \rightarrow 3I_3^- + 6OH^- \quad (1)$$

The solution at first is optically transparent above 330 nm; however upon exposure to UV irradiation at 254 nm the photoproduct triiodide ion (I_3^-) that is formed exhibits a strong absorption at λ = 352 nm (A_{352}) with molar absorption coefficient ε_{352} = 27,636 $M^{-1}\,cm^{-1}$ in a 0.6 M KI/0.1 M KIO_3 solution (Stefan et al., 2001). The KI/KIO_3 actinometry stock solution was prepared according to Rahn (1997). In short, 100 mL of the KI/KIO_3 actinometry stock solution was prepared by weighing out 9.96 g of KI, 2.14 g of KIO_3 and 0.381 g of sodium tetraborate ($Na_2B_4O_7{\cdot}10H_2O$). The quantum yield of this actinometer (ϕ) was taken as 0.64 at 254 nm and 20.7 °C. Values of the blank actinometer prior to UV exposure (i.e., the unirradiated control) was taken as A_{352} (blank). After UV exposure the actinometer was immediately transferred to a quartz cuvette with 1 cm pathlength and absorbance was measured at 352 nm, and labeled A_{352} (sample). Absorbance measurements were performed with a *UV–Vis* dual beam spectrophotometer (Varian, Model Cary 100BIO). The ideal exposure time (s) of the actinometer in a well mixed petri dish under 254 nm LP collimated beam apparatus was found empirically to avoid saturation of the actinometer.

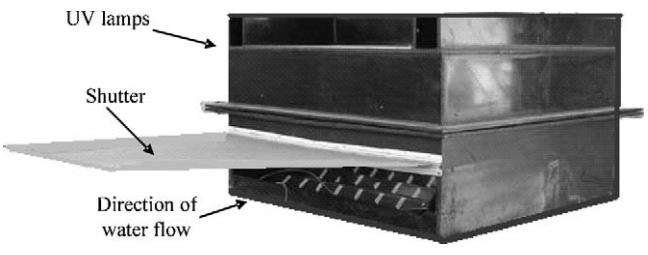

Fig. 3. Photograph of UV reactor.

The fluence rate (E^0) with actinometer was calculated by:

$$E^0 = \frac{[A_{352}(\text{sample}) - A_{352}(\text{blank})] \times V(\text{mL})}{\text{Area}\,(\text{cm}^2) \times \text{Exposure time}\,(\text{s}) \times \phi \times \varepsilon_{352}} \times U\,(\text{mW cm}^{-2}) \quad (2)$$

where U is the constant used to convert einsteins into conventional UV fluence units of mJ at 254 nm wavelength (4.72×10^8 mJ $Einstein^{-1}$), V is the volume of the actinometer inside the vessel and Area relates to the cross-sectional area.

2.4. UV reactor testing

Fluence rate distribution in the UV reactor was obtained by the spherical actinometry method. Spherical actinometry is a technique whereby an actinometer is placed inside a quartz vessel, which can then "record" photons coming from all directions. Each sphere was measured for exact volume by the increase in weight when filled with water. The cross-sectional area of each sphere was calculated based on the volume and assuming spherical geometry. The spherical quartz vessels were approximately 0.9–1.2 cm in diameter, with a volume of 0.4–0.8 mL and a cross-sectional area (area which intercepts the radiant energy) of 0.6–0.9 cm^2. Spheres were composed of the sphere vessel that holds the liquid and a narrow extending stem through which the liquid is filled into or withdrawn out of the sphere and which also serves as a holding location. The spherical vessels were attached at various fixed (X, Y, Z) positions according to Fig. 4 on a grid at different locations in the reactor's water tray.

Prior to each exposure, the lamp was warmed up to a constant irradiance. A manual shutter between the UV lamps and the grid was used to adjust the UV exposure level. After exposure, the grid was removed, and the actinometer was withdrawn from the spheres with a Pasteur pipette. The actinometer was transferred to 1 cm cuvettes for absorbance measurements of the photoproduct at λ = 352 nm for each X, Y, Z location tested. The UV fluence rate was initially measured in a dry system (without water), at the assumed water surface. A total of twenty-one X, Y measurements for each X, Y location, with two repetitions at each location, resulted in a total of 42 measurements (n = 42) at the water surface height.

2.5. Calculation of absorption coefficient

Absorbance is characterized by the decrease in the amount of incident light as it passes through a water sample over a specified distance or path length. UV absorbance of a substance varies with the wavelength (λ) of the light. The absorption coefficient (α)

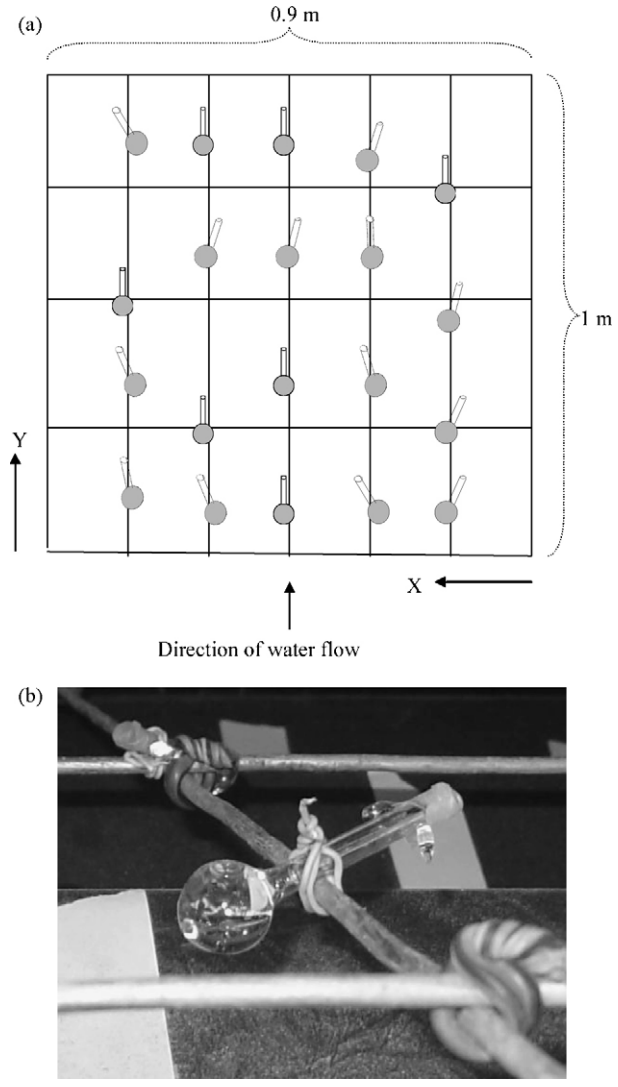

Fig. 4. (a) Schematics of a grid with possible locations of spherical actinometers attached on various *X*, *Y* locations. Where *X* is the distance from the right wall of the tray and *Y* is the distance from the water entry to the tray (top); (b) a close-up photograph of a spherical actinometer attached to a metal grid (bottom).

(cm^{-1}) of a homogeneous sample is obtained by absorbance measurements, as follows:

$$\alpha\,(cm^{-1}) = \frac{A \cdot \ln(10)}{l} = \frac{A \cdot 2.303}{l} \quad (3)$$

where A is the absorbance measured via *UV–Vis* spectrophotometer (Cary Bio100, Varian, Inc., Palo Alto, CA); l is the path length of the cuvette which is equal to 1 cm (in this case) (detailed derivation in Linden and Darby, 1998).

2.6. Calculation of UV irradiance (fluence rate) and dose (fluence)

The radiometer sensor provides a measure of the incident irradiance on the water surface at the center of the beam. In addition using actinometers can also provide a measure of the incident irradiance (as detailed above). The average fluence rate is obtained by multiplying the incident irradiance with a correction factors that account for the decrease in irradiance arising from absorption as the beam passes through the water. The average UV irradiance (or fluence rate in a completely mixed disinfection system) is defined as:

$$E_a = E_0 \times \frac{(1 - e^{-\alpha h})}{\alpha h} \quad (4)$$

where E_0 is the incident irradiance on the water surface, mW cm^{-2}; E_a is the average irradiance or fluence rate in bulk water, mW cm^{-2}; h is the vertical path length (cm) of the water.

The average UV dose or fluence to which the microorganisms are exposed (Eq. (5)) can be calculated as a factor of the average UV irradiance (E_a) and exposure time (t).

$$\text{UV Dose}\,(mJ\,cm^{-2}) = E_a\,(mW\,cm^{-2}) \times t\,(s) \quad (5)$$

2.6.1. The impact of water depth in the UV reactor

In order to determine the effect of reactor's water depth on the UV fluence rate, the spherical actinometry method was conducted in the fish tank water. The quartz spheres were submerged at different depths in fish tank water.

2.6.2. The impact of flow rate in the UV reactor

After installing the reactor in the RAS, water level in the reactor was measured in different water flow rates. Flow rate (Q) was calculated from the time needed to fill a water tank of known volume (V = 710.5 L).

2.7. Bacteriological measurements for both CBA and UV reactor

The bacterial concentrations (of non-irradiated and UV irradiated samples) were determined after serial 10-fold dilutions, using the pour plate technique. A water sample collected from the fish tank at a known volume was mixed with 15 mL of warm liquid tryptic soy agar (TSA). The agar was transferred to a petri dish and, to prevent spreading of swarming bacteria on the agar surface, after solidification the medium was covered by a layer of plain agar. The plates were incubated for 3 days at 24 °C for colony counting. Bacterial colonies that developed were counted under a stereomicroscope. The concentration of the microorganisms as colony forming units (CFU) per mL was obtained by counting the number of colonies divided by the water volume. Only plates carrying 30–300 colonies were used for counting.

Laboratory UV exposures were carried out using a low pressure (LP) bench scale UV collimated beam apparatus (CBA). The UV radiation was directed through a circular opening (collimated tube) to provide incident radiation normal to the surface of the water test suspension. Aliquots of fish tank water with indigenous microorganisms were placed in a glass dish and irradiated while stirring to a range of UV fluences. Mean concentration (CFU mL^{-1}) of microorganisms without UV exposure was taken as the initial concentration, N_0, while the arithmetic mean concentration per fluence was N_d. UV fluence was obtained by multiplying the average fluence rate by the exposure time. Average UV dose was determined according to the procedure described in Bolton and Linden (2003). The $\log_{10}$ transformation for N_0/N_d was plotted as a function of the UV fluence, and dose–response curves were developed. Regression analysis was performed on all the data fields used to fit the linear sections of the log inactivation curve.

The field experiment was performed with the UV reactor installed in the RAS between the biofilter and the fish tank (see Fig. 1). Samples were taken from the inlet water and the outlet effluent of the reactor. Data were analyzed with JMP IN® 5.1 statistical software (SAS Institute Inc., Cary, NC, USA) and results were presented as means ± SE.

2.8. Water quality measurements

Total suspended solid (TSS) is the portion of total solids (TS) retained by a filter (usually 0.45 μm but up to 2.0 μm) measured after being dried (Metcalf and Eddy, 2004). Total suspended solids (TSS) were measured by filtering a sample the RAS water through pre weighted paper-filter with 0.7 μm pore size. The filter was washed with deionized water in order to discard the seawater salts, dried at 105 °C for 1 h and re-weighed. Turbidity was measured by turbidimeter (Model 2020, LaMotte Company, MD, USA).

3. Results and discussion

3.1. Water quality

Fig. 5 illustrates absorbance measurements of a representative sample of seawater collected at the entrance of the fish tank and from the recirculating fish tank water (RAS) as a function of wavelengths from 200 to 400 nm at 1 nm intervals with the baseline of the instrument adjusted with deionized water. The water absorbance and transmittance in parenthesis (termed UVT) at 253.7 nm from the RAS is 0.072 (UVT 85%) and for seawater is 0.010 (UVT 98%). This results in an absorption coefficient of $\alpha = 0.166\ cm^{-1}$ and $0.023\ cm^{-1}$, respectively. The water in the RAS is expected to accumulate dissolved and particulate organics and result in higher absorbance than seawater, especially at wavelength below 250. When UV light is absorbed in the water matrix, it is no longer available to eliminate microorganisms as these wavelengths may not be available for UV disinfection (USEPA, 2006). Examples for compounds that absorb in the UV range are: (a) iron compounds in water that lower water transmittance, thus increase the UV dose required or result in poorer UV disinfection (Cairns et al., 1993); (b) organic substances as humics in water that absorb light in the UV and visible range (Frimmel, 1998).

The UV reactor was installed in the RAS between the fish tank and the biofilter (Fig. 1). The most important design parameter for UV facilities is the ultraviolet transmittance (UVT), and a minimum UVT of 88% was chosen for UV reactor validation for many validation tests (USEPA, 2006). Particle count/characteristics and UVT of the water can be controlled by unit processes and chemical addition upstream of UV reactors thereby optimizing the design, costs and performances of the UV reactor.

TSS concentrations for outlet of the solid filtration unit were 5–15 mg L^{-1}, with more than 50% of the TSS measuring less than 15 μm, with an overall filtration efficiency of 56%. Average TSS values in the RAS water were 9.2 ± 0.4 mg L^{-1} TSS. Average turbidity values in the fish tank were 3.7 ± 0.2 NTU. Both total solids and turbidity are lumped parameters that do not provide any information on size or distribution of the individual particles in the water, which can be obtained by particle size analyzers.

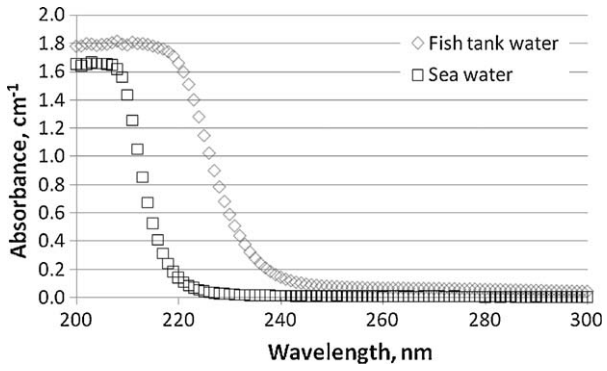

Fig. 5. Absorbance measurements of seawater collected at the entrance of the fish tank and from the recirculating fish tank water (RAS) as a function of wavelength.

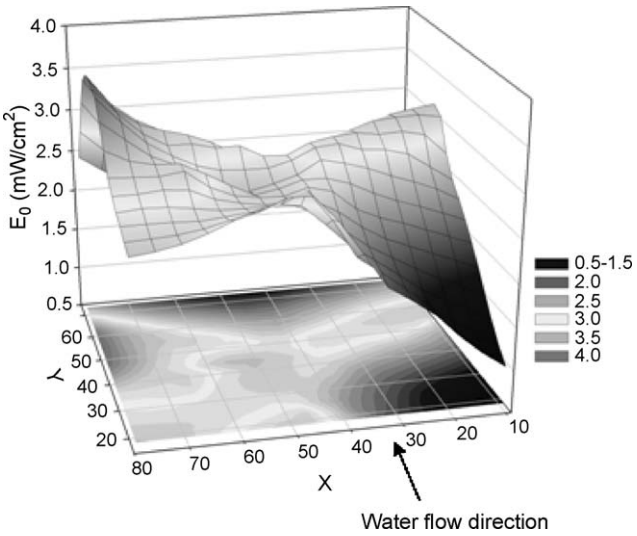

Fig. 6. Three-dimensional surface plots of fluence rate in the UV reactor measured with spherical actinometer method in air at the surface of the test water (water depth = 0).

3.2. Fluence rate in the UV reactor surface and at various depths

Fig. 6 illustrates the three-dimensional surface plot of fluence rate in the UV reactor measured with spherical actinometer method in air. Fluence rate was measured according to Eq. (2), and based on twenty-one *X*, *Y* points, where *X* and *Y* are the axis which represent the distances in the tray as detailed in Fig. 4. The fluence rate E^0 slightly peaks at the center of the lamp and to some extent decreases away from the center. In addition, results show that the distribution is not totally homogenous at the tray. Normally distributed population was verified by the Shapiro–Wilk test population. Exposure times in the reactor were kept short, at 10 s. The average fluence rate that is obtained at a distance of 37.5 cm from the lamps is 2.562 ± 0.954 mW cm^{-2}. The fluence rate in three dimensions is interesting, as it can be used for design purposes and for improving the present reactor design. For example, the decay of fluence rate at certain zones might be due to the reactor's wall absorbance or reflector design.

In order to determine the effect of water depth on the UV fluence rate, the same experiment was conducted in fish tank water. The

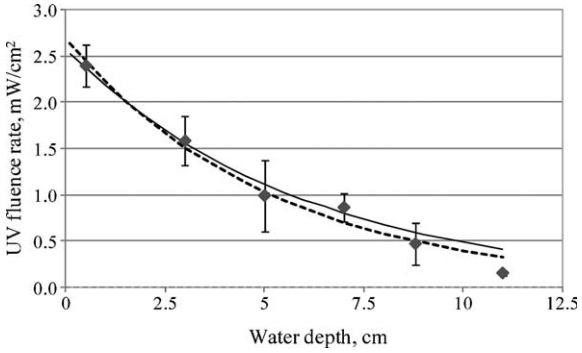

Fig. 7. UV fluence rate decay in fish tank water as a function of water depth: dots represent UV fluence rates measured, the dashed line represents the best-fit regression to the data ($E_0 = 2.69$ mW cm^{-2} and absorption coefficient of 0.191 cm^{-1}, as detailed in Eq. (6)), solid line is the theoretical modeled fluence rate exponential decay ($E_0 = 2.562$ mW cm^{-2} and absorption coefficient of 0.166 cm^{-1}, as detailed in Eq. (7)).

quartz spheres were submerged at different depths in the water. Fig. 7 illustrates the UV fluence rate decay in fish tank water as a function of water depth. Depth measurements were conducted for an average of four spheres for each depth at *X*, *Y* locations (in cm) of (7.5, 60); (60.5, 49); (54.5, 50) and (42, 61). Irradiance measurements in the water conducted with the spherical actinometers showed an exponential decay with the increase in water depth, as expected. In the figure, the dots represent UV fluence rates as measured in the UV reactor with fish tank water, while the dashed line represents the best-fit regression to the data (as detailed in Eq. (6) below) using GraphPad Prism software, where the following optimal parameters were obtained: $E_0 = 2.69\ \text{mW/cm}^2$ and absorption coefficient of 0.191 1 cm^{-1}. The solid line is the theoretical modeled fluence rate exponential decay considering the following parameters: the data obtained empirically for the average irradiance at the surface of the test water (water depth = 0) $E_0 = 2.562 \pm 0.954\ \text{mW cm}^{-2}$ and $A_{254} = 0.072$ or $\alpha = 0.166\ \text{cm}^{-1}$ for the absorbance at 254 nm (as detailed in Eq. (7) below). It can be observed that the best-fit regression (Eq. (6)) describes the theoretical modeled fluence rate exponential decay (Eq. (7)) with good agreement. The last data point obtained with the spherical actinometer is lower than the modeled line. This may occur as at higher depth of water, possibly settled particles have interfered with UV light penetration through the water, as the water in the tray was not mixed during experiment.

$$E' = 2.6908 \times e^{(-0.191 \cdot X)}; \quad R^2 = 0.9283 \tag{6}$$

$$E' = 2.562 \times e^{(-0.166 \cdot X)} \tag{7}$$

3.3. UV dose as a function of flow rate in the UV reactor

Measurements of the water flow rate were conducted by varying the water pumped by an airlift pump and measuring the time of filling a known tank volume. Calibration of water height (h) of flowing water in the tray of the UV reactor with the water flow rate (Q) showed a linear relationship, described in Eq. (8).

$$Q\ (\text{m}^3\ \text{h}^{-1}) = 2.47 \cdot h\ (\text{mm}) - 195.42; \quad R^2 = 0.99 \tag{8}$$

where Q = water flow rate through the UV reactor ($\text{m}^3\ \text{h}^{-1}$); h = water depth in the UV reactor (mm).

When calculating the average UV irradiance (Eq. (4)) it is necessary to account for the decrease in irradiance arising from absorption as the beam passes through the water (Bolton and Linden, 2003). The average UV dose or fluence to which the microorganisms are exposed (Eq. (5)) for any water absorbance can be calculated as a factor of the average UV irradiance at a certain depth (see Fig. 7) and the residence time in the tray. The residence time is a factor of the system volume divided by the flow, which can be calculated using Eq. (8). The volume is a factor of the rectangular base which includes a tray 1 m wide and 0.9 m long (Fig. 1) and the water depth (h) in the tray.

Finally the UV dose was determined according to Eq. (9) as follows:

$$\begin{aligned}\text{UV Dose}\ (\text{mJ cm}^{-2}) &= E_a(\text{mW/cm}^2) \times (V/Q) \\ &= E_0 \times \frac{(1 - e^{-\alpha \cdot 0.1 \cdot h})}{\alpha \cdot} \times \frac{l \cdot w \cdot \cdot 36}{Q};\ E_0 \\ &= 2.562\ \text{mW cm}^{-2};\ \alpha = 0.166\ \text{cm}^{-1}\end{aligned} \tag{9}$$

where h: water depth in the tray, $f(Q)$, mm; w: tray width, m; l: tray length, m.

Fig. 8 illustrates the UV dose as a function of the water flow rate in the tray based on calculated model (Eqs. (8) and (9)) assuming exponential UV fluence decay with water depth. Thus, measurements of the exponential decay of irradiance in the water with the increase in water depth, using spherical actinometry, can be used to estimate the reactor's UV dose at different water flow rates.

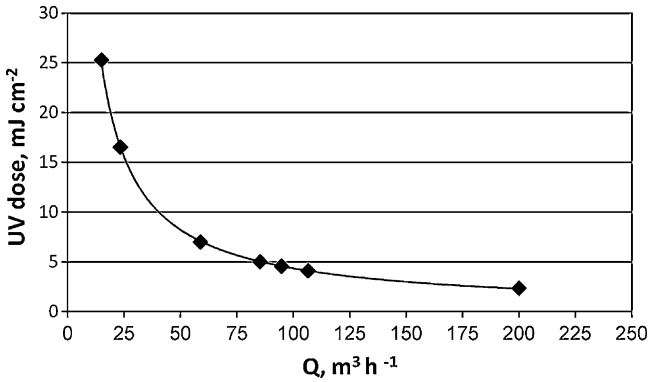

Fig. 8. UV dose vs. water flow rate (Q) for the UV reactor (based on Eqs. (8) and (9), where $\alpha = 0.166$; $w = 1$ m; $l = 0.9$ m; $h = f(Q)$; $E_0 = 2.562\ \text{mW cm}^{-2}$).

3.4. Dose–response curves

Eq. (10) describes the inactivation of disperse bacteria in completely mixed batch reactor. The one hit model assumes that a single harmful event (hit) is sufficient to inactivate a biological unit (Harm, 1980). The dose–response curve is computed as log reduction ($\log_{10} N_0/N_D$) as a function of UV dose and shows first order kinetics as a function of UV dose.

$$\log\left(\frac{N_0}{N_D}\right) = kI_a t = kD \tag{10}$$

where N_D = total number of surviving bacteria at UV dose D; N_0 = total number of bacteria before UV application (at time $t = 0$); k = inactivation rate coefficient, $\text{cm}^2\ \text{mJ}^{-1}$; I_a = average irradiance of UV light in bulk solution, mW cm^{-2}; t = exposure time in seconds, s; D = UV dose or fluence, mJ cm^{-2}.

Fig. 9 illustrates the log inactivation of heterotrophic microorganisms from the RAS water as a function of UV fluence, using the collimated beam apparatus (CBA). The data shown are related to the total bacteria counts that grew in the TSA, which may represent a small fraction of the bacteria actually present in the water samples. No attempt to identify the bacteria counted was done. However, based on experience, most such bacteria at the NCM belong in the *Vibrionaceae* family (*Vibrio* spp.). In general, survival of bacteria dropped significantly as the UV dose increased and then stabilized. Initially, a first order linear relationship was observed between the microorganisms logarithmic survival rate and UV fluence between 0 and 13 mJ cm^{-2}, with an approximate 2.2-log reduction (99%), followed by a reduced inactivation rate with increasing UV fluence termed tailing.

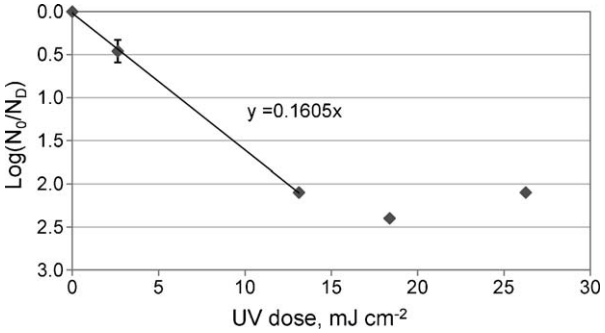

Fig. 9. Dose–response curve using a bench scale collimated beam apparatus (CBA) for indigenous microorganisms.

The transition between the 1st order section and the tailing is generally not precisely discernable (Mamane-Gravetz and Linden, 2005). Tailing implies a residual of microorganisms present in the water even at very high UV fluences, which could result in a public health concern. Tailing was observed in many UV disinfection studies typically of wastewater effluents. For example, a transition region was observed between the linear and tailing zone for coliforms on the interface of particles without a direct pathway of light that reduces inactivation efficacy (Loge et al., 2001). It is complex, however, to predict the tailing phenomenon mathematically (Chiu et al., 1999).

In case where particles appear in water, filtration should be evaluated. Liltved and Cripps (1999) suggested filtration of seawater for aquacultural purposes combined with UV disinfection to avoid transmission of fish pathogenic bacteria from sea to land-based aquaculture such as salmonid hatcheries. A 50 μm filter of the pumped seawater followed by a UV dose of 22 mJ cm^{-2} can achieve more than 5 logs reductions indicating that after filtration the majority of the bacterial counts were single cells or cells attached to small fragments. However, RAS's water that contains large fraction of small size solids (55–85% of the suspended solids at size less than 15 μm, Mozes et al., 2003) additional filtration would be costly, and therefore tailing may be unavoidable.

Turbidity measurements do not provide information regarding the extent of association of microorganisms with particles; however suspended solid concentration can be correlated to some extent with aggregation and is site specific. Various studies did not find a consistent relationship between TSS and UV disinfection performance (Qualls et al., 1983; Madge and Jensen, 2006). In this study the TSS values and turbidity were around 10 mg/L and 4 NTU, respectively, suggesting that tailing may be due to particle-microbe association.

Because it is difficult to directly measure the UV fluence delivered in a UV disinfection reactor, the current method to validate a UV reactor is to measure the inactivation of a microbial surrogate through a UV reactor and back-calculate the delivered UV fluence using the biodosimetry method. Although conventional validation testing of UV reactors use cultured microorganisms spiked into test water flowing through a reactor, still in unfiltered water supplies alternative indigenous indicators such as naturally occurring aerobic spores (Mamane-Gravetz and Linden, 2004) can be used for validation testing of UV reactor performance. Thus to determine the UV dose in the reactor, samples were taken from the inlet water and the outlet water of the UV reactor. The recirculation water flow rate and residence time were 105.8 $m^3\ h^{-1}$ and 3.44 s, respectively. Fig. 10 illustrates bacteria concentration in water flowing in and out of the UV reactor.

Bacteria concentration in the inlet water of the UV reactor was significantly higher than the bacteria concentration in the outlet water (1548.3 ± 329.4 vs. 821.3 ± 292.7 counts/mL, respectively; *t*-test, $p < 0.05$). Percent Removal Efficiency is calculated by Eq. (11)

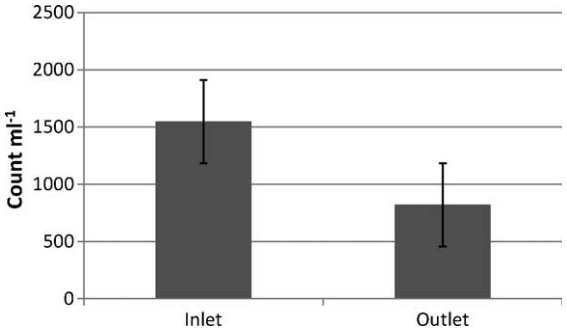

Fig. 10. Bacteria concentration in water flowing in and out of the UV reactor.

where C_i is inlet microbial concentration of raw sample and C_e is microbial concentration at the outlet.

$$\%RRE = \left(\frac{C_i - C_e}{C_i}\right) \cdot 100 \quad (11)$$

Using this equation results in about 50% reduction in microbial concentration, when the water flow was about 100 $m^3\ h^{-1}$. It is apparent that decrease in water flow will increase the UV dose applied to the water and consequently increase reduction in bacterial counts.

Reduction in bacterial count corresponded to 0.3 log reduction. Log survival of 0.3 at the UV reactor installed in the RAS, was used to back calculate the average UV dose, and resulted in a dose of ~2 mJ cm^{-2} based of the CBA results (according to Fig. 9). Using Eq. (9) as other means of calculation, a flow of about 100 $m^3\ h^{-1}$ correlates to a calculated UV dose of ~4 mJ cm^{-2} (as demonstrated in Fig. 8), which is higher than the average dose obtained by the re-calculation approach using the CBA, but still is at the same order of magnitude. The differences in UV dose are probably due to various interference factors not considered, such as fine air bubbles that are carried with the water pumped by the air-lifts in the full scale RAS.

According to the USEPA UV disinfection guidance manual UV doses of 1–10 mJ cm^{-2} achieve 90–99.9% and more inactivation of numerous water pathogenic bacteria and protozoa (USEPA, 2003). Table 1 summarizes the UV sensitivity of fish bacterial pathogens in water taken from the USEPA UV disinfection guidance manual (2003).

The results suggest that flow rates of 100 $m^3\ h^{-1}$, with the given fluence rates will deliver UV doses of 2–4 mJ cm^{-2} when using 30 W LP lamps. As a safety measure the recommended lamps would be of higher power (55 W each), almost doubling the dose. The given fluence should be sufficient to inactivate at least 50% (according to the measured results in full scale) and with the improved lamps even 90–99.9% (according to Table 1) of various bacteria. This relatively low doses and low expected reduction of pathogens is expectable for the case of low UVT (85%) and under the concept of avoiding further filtration and pressurizing the water in the LH-RAS.

The cost benefit analysis for different UV instruments considered investment and operational costs. The investment cost was translated to capital return cost and the operational costs included the energy required for lamps, the maintenance costs of replacing lamps (according to its lifetime period) and the cost of pumping head loss on the UV instrument itself. In other UV instruments that are pressurized additional cost of pumping, at a head of 1 atm, was added to the operational cost. On the benefit side the treated water flowing through the instrument was considered. The cost of the LP open flow UV treatment was calculated to be US$ Cent 0.12 per 1 treated m^3 versus a cost of US$ Cent 0.67 to 1.07 per 1 treated m^3 in other UV instruments (pressurized). Further investigation on quantifying the benefit of UV output in RAS is required, but at the given constrains of turbidity and water pressure this analysis support the use of the LP open flow UV in the LH RAS.

A study by Liltved et al. (1995) showed rapid inactivation of three fish pathogenic bacteria (*Vibrio anguillarum*, *Vibrio salmonicida* and *Yersinia ruckeri*) in brackish water. A UV dose of

Table 1
UV doses needed for inactivation of common fish pathogens (USEPA, 2003).

Microorganism	Type	UV dose (mJ cm^{-2})			
		1-log	2-log	3-log	4-log
Aeromonas hydrophila	Bacterium	1.1	2.6	3.9	5.0
Vibrio cholera	Bacterium	0.8	1.4	2.2	2.9
Streptococcus faecalis	Bacterium	6.6	8.8	9.9	11.0

2.7 mJ cm^{-2} resulted in 99.999% (5 log) reduction of viable counts for all bacteria using a LP lamp, with a near linear response in the dose–response curve. However, Atlantic halibut nodavirus (AHNV), infectious pancreatic necrosis virus (IPNV) and infectious salmon anaemia virus (ISAV) required 105, 246, and 7.7 mJ cm^{-2} for 3-log of inactivation in seawater, respectively (Liltved et al., 2006). Therefore, this reactor may achieve partial disinfection of sensitive bacteria and not necessarily viruses and other UV resistant microorganism. However, because water is treated and reused repeatedly in the RAS, (recirculation rate is typically 1 exchange per hour), Summerfelt et al. (2009) showed that the mean daily ozone disinfectant demand was lower than what is typically required to disinfect surface water in a single pass treatment. This possibly has implications also on UV doses needed for controlling pathogenic bacteria proliferation of recycled water in systems such as the RAS that are treated many times daily, compared to disinfection of drinking water. Photoreactivation of fish pathogenic bacterium should be taken into consideration when assessing the efficiency of post-UV irradiation subjected to artificial visible light illumination and sunlight for treatment of aquacultural water and surface water (Liltved and Landfald, 1996, 2000). Research has also shown that, to ensure permanent inactivation and prevent the recovery of microorganisms following exposure to UV, a MP lamp is necessary as they damage not only on cellular DNA, but also enzymes and other molecules responsible for DNA light repair (Oguma et al., 2002; Zimmer and Slawson, 2002; Kalisvaart, 2004). However, aiming at reducing operational costs, only a LP lamp was considered.

4. Summary and conclusions

This study examined the effectiveness of an open, LP, UV reactor for water treatment in a LH-RAS. The UV reactor's output was evaluated by measuring the fluence rate distribution and average UV fluence rate delivered to the water surface using spherical chemical actinometry. UV fluence rate distribution in the reactor's tray is fairly even. The average UV fluence rate measured in dry conditions was 2.562 ± 0.954 mW cm^{-2}. Measurements of the exponential decay of irradiance in the water with the increase in water depth were used to estimate the reactor's UV dose at different water flow rates. The results suggest that flow rates of 100 m^3 h^{-1}, with the given fluence rates will deliver low UV doses of ~4 mJ cm^{-2} when using 30 W LP lamps for controlling to some extent pathogenic bacteria proliferation in recycled RAS system. Because water is treated and reused repeatedly in the RAS, the mean daily disinfectant used for controlling pathogenic bacteria proliferation may be lower than what is typically required to disinfect surface water in a single pass treatment. Nevertheless, to practically apply this type of LP UV disinfection reactor in a RAS, it would be advisable to construct this system in water with highest transmittance possible, lamps with higher output and with flow rates that allow sufficient exposure time for disinfection and higher UV doses.

Acknowledgments

We wish to thank the NCM's aquaculture engineering staff: Helena Chernov, Michael Pediuk and Eng. Yuval Alfiya for their help and technical support; Guy Shavit from "Ardag" fish farm, for kindly providing data on other UV systems, and Yair Hagani at Kora 1980 Ltd. (Israel), for kindly supplying the UV reactor.

References

Bolton, J.R., 2001. Ultraviolet Application Handbook, 2nd ed. Bolton Photosciences.
Bolton, J.R., Linden, K.G., 2003. Standardization of methods for fluence (UV Dose) determination in bench-scale UV experiments. Journal of Environmental Engineering 129, 209–215.
Cairns, W., Sakamoto, G., Comair, C., Gehr, R., 1993. Assessing UV disinfection of a physico-chemical effluent by medium pressure lamps using a collimated beam and pilot plant. In: Proc. "Planning, Design & Operation of Effluent Disinfection Systems", Water Environment Federation Specialty Conf., Whippany, NJ.
Chiu, K., Lyn, D.A., Savoye, P., Blatchley, E.R., 1999. Integrated UV disinfection model based on particle tracking. Journal of Environmental Engineering 125, 7–16.
Clancy, J.L., Bukhari, Z., Hargy, T.M., Bolton, J.R., Dussert, B.W., Marshell, M.M., 2000. Using UV to inactivate Cryptosporidium. Journal of American Water Works Association 92, 97–104.
Craik, S.A., Weldon, D., Finch, G.R., Bolton, J.R., Belosevic, M., 2001. Interactivation of *Cryptosporidium parvum* oocysts using medium- and low-pressure ultraviolet radiation. Water Research 35, 1387–1398.
Crittenden, J.C., Trussell, R.R., Hand, D.W., Howe, K.J., Tchobangolous, G., 2005. Water Treatment: Principles and Design, 2nd ed. John Wiley and Sons, New Jersey.
Frimmel, F.H., 1998. Characterization of natural organic matter as major constituents inaquatic systems. Journal of Contaminant Hydrology 35, 201–216.
Haider, T., Sommer, R., Knasmuller, S., Eckl, P., Pribil, W., Cabaj, A., Kundi, M., 2002. Genotoxic response of Austrian groundwater samples treated under standardized UV (254 nm) disinfection conditions in a combination of three different bioassays. Water Research 36, 25–32.
Harm, W., 1980. Biological Effects of Ultraviolet Radiation. Cambridge, Eng.; Cambridge University Press, New York.
Hatchard, C.G., Parker, C.A., 1956. A new sensitive chemical actinometer II. Potassium ferrioxalate as a standard chemical actinometer. Proceedings of the Royal Society A235, 518–536.
Jortner, J., Levine, R., Ottonlenghi, M., Stein, G., 1961. The photochemistry of the iodide ion in aqueous solution. The Journal of Physical Chemistry 65, 1232–1238.
Kalisvaart, B.F., 2004. Re-use of wastewater: preventing the recovery of pathogens by using medium-pressure UV lamp technology. Water Science and Technology 50, 337–344.
Klas, S., Mozes, N., Lahav, O., 2006. Conceptual, stoichiometry-based model for single-sludge denitrification in recirculating aquaculture systems. Aquaculture 259, 328–341.
Kornmueller, A., 2007. Review of fundamentals and specific aspects of oxidation technologies in marine waters. Water Science and Technology 55, 1–6.
Kuhn, H.J., Braslavsky, S.E., Schmidt, R., 1989. Chemical actinometry. Pure and Applied Chemistry 61, 187–210.
Leonard, N., Blancheton, J.P., Guiraud, J.P., 2000. Populations of heterotrophic bacteria in an experimental recirculating aquaculture system. Aquacultural Engineering 22, 109–120.
Liltved, H., Cripps, S.J., 1999. Removal of particle-associated bacteria by prefiltration and ultraviolet irradiation. Aquaculture Research 30, 445–450.
Liltved, H., Hektoen, H., Efraimsen, H., 1995. Inactivation of bacterial and viral fish pathogens by ozonation or UV radiation in water of different salinity. Aquacultural Engineering 14, 107–122.
Liltved, H., Landfald, B., 1996. Influence of liquid holding recovery and photoreactivation on survival of ultraviolet-irradiated fish pathogenic bacteria. Water Research 30, 1109–1114.
Liltved, H., Landfald, B., 2000. Effects of high intensity light on ultraviolet-irradiated and non-irradiated fish pathogenic bacteria. Water Research 34, 481–486.
Liltved, H., Vogelsang, C., Modahl, I., Dannevig, B.H., 2006. High resistance of fish pathogenic viruses to UV irradiation and ozonated seawater. Aquacultural Engineering 34, 72–82.
Linden, K.G., Shin, G.A., Faubert, G., Cairns, W., Sobsey, M.D., 2002. UV disinfection of *Giardia lamblia* in water. Environmental Science and Technology 36, 2519–2522.
Linden, K.G., Darby, J.L., 1998. Ultraviolet disinfection of marginal effluents: determining ultraviolet absorbance and subsequent estimation of ultraviolet intensity. Water Environment Research 70, 214–223.
Loge, F.J., Bourgeous, K., Emerick, R.W., Darby, J.L., 2001. Variations in wastewater quality influencing UV disinfection performance: relative impact on filtration. Journal of Environmental Engineering 127, 832–837.
Losordo, T.M., Masser, M.P., Rakocy, J., 1998. Recirculating aquaculture tank production systems—an overview of critical considerations, SRAC Publication No. 451 (aqua.ucdavis.edu/dbweb/outreach/aqua/451RFS.PDF).
Madge, B.A., Jensen, J.N., 2006. Ultraviolet disinfection of fecal coliform in municipal wastewater: effects of particle size. Water Environment Research 78, 294–304.
Mamane, H., 2008. Impact of particles on UV disinfection of water and wastewater effluents: a review. Reviews in Chemical Engineering 24, 67–157.
Mamane-Gravetz, H., Linden, K.G., 2004. UV disinfection of indigenous aerobic spores: implications for UV reactor validation in unfiltered waters. Water Research 38, 2898–2906.
Mamane-Gravetz, H., Linden, K.G., 2005. The relationship between physiochemical properties, aggregation, and UV inactivation of isolated indigenous spores in water. Journal of Applied Microbiology 98, 351–363.
Metcalf, Eddy, 2004. Wastewater Engineering Treatment and Reuse, 4th edition. Mc-Graw Hill.
Mozes, N., Eshchar, M., Conijeski, D., Fediuk, M., Ashkenazy, A., Milanez, F., 2003. Field report: marine recirculating systems in Israel—performance, production cost analysis and rational for desert conditions. The Israeli Journal of Aquaculture-Bamidgeh 55, 243–257.
Oguma, K., Katayama, H., Ohgaki, S., 2002. Photoreactivation of *Escherichia coli* after low- or medium-pressure UV disinfection determined by an endonu-

clease sensitive site assay. Applied and Environmental Microbiology 68, 6029–6035.
Qualls, R.G., Flynn, M.P., Johnson, D., 1983. The role of suspended particles in ultraviolet disinfection. Journal of the Water Pollution Control Federation 55, 1280–1285.
Rahn, R.O., 1997. Potassium iodide as a chemical actinometer for 254 nm radiation: use of iodate as an electron scavenger. Photochemistry and Photobiology 66, 450–455.
Rahn, R.O., Xu, P., Miller, S.L., 1999. Dosimetry of room-air germicidal (254 nm) radiation using spherical actinometry. Photochemistry and Photobiology 70, 314–318.
Sharrer, M.J., Summerfelt, S.T., 2007. Ozonation followed by ultraviolet irradiation provides effective bacteria inactivation in a freshwater recirculating system. Aquacultural Engineering 37, 180–191.
Shin, G.A., Linden, K.G., Arrowood, M.J., Sobsey, M.D., 2001. Low-pressure UV inactivation and DNA repair potential of *Cryptosporidium parvum* oocysts. Applied and Environmental Microbiology 67, 3029–3032.
Singer, P., Reckhow, D., 1999. A Handbook of Community Water Supplies. McGraw-Hill, Inc., New York.
Stefan, M.I., Rahn, R.O., Bolton, J.R., 2001. Use of iodide/iodate actinometer together with spherical cells for determination of the fluence rate distribution in UV reactors: validation of the mathematical model. In: Proceedings of the 1st International Congress on Ultraviolet Technologies. International Ultraviolet Association.
Summerfelt, S.T., 2003. Ozonation and UV irradiation—an introduction and examples of current applications. Aquacultural Engineering 28, 21–36.
Summerfelt, S.T., Sharrer, M.J., Tsukuda, S.M., Gearheart, M., 2009. Process requirements for achieving full-flow disinfection of recirculating water using ozonation and UV irradiation. Aquacultural Engineering 40, 17–27.
U.S. Environmental Protection Agency (USEPA), 2003. Ultraviolet Disinfection Guidance Manual, EPA 815-D-03-007. Office of Water, Washington, DC.
U.S. Environmental Protection Agency (USEPA), November 2006. Ultraviolet Disinfection Guidance Manual Final, EPA 815-R-06-007. Office of Water, Washington, DC.
Zimmer, J.L., Slawson, R.M., 2002. Potential repair of *Escherichia coli* DNA following exposure to UV radiation from both medium- and low-pressure UV sources used in drinking water treatment. Applied and Environmental Microbiology 68, 3293–3299.